KERNEL-BASED METHODS FOR SOLVING SURFACE PARTIAL DIFFERENTIAL EQUATIONS

MENG CHEN[1] & LEEVAN LING[2]
[1]Department of Mathematics, Nanchang University, China
[2]Department of Mathematics, Hong Kong Baptist University, Hong Kong

ABSTRACT
A convergence analysis technique in our previous work is extended to various theoretically proven convergent kernel-based least-squares collocation methods for surface elliptic equation, projection methods for surface elliptic equation, and recently for surface parabolic equations. These partial differential equations (PDEs) on surfaces closely resemble their Euclidean counterparts, except that the problem domains change from bulk regions with a flat geometry to some manifolds, on which curvatures plays an important role in the physical processes. We do not focus on proofs in this paper, but on implementation details instead. First, we present an embedding formulation to solve a surface PDE in a narrow-band domain containing the surface. Next, we present another extrinsic projection formulation that works solely on data points on the surface. Lastly, we solve surface diffusion problem using kernel and the method of lines.
Keywords: convergence estimate, least-squares, Kansa method, partial differential equations on manifolds, surface diffusion.

1 INTRODUCTION

All theories we review in this paper require Sobolev space-reproducing kernel $\Phi : \mathbb{R}^d \times \mathbb{R}^d \to \mathbb{R}$ whose Fourier transform decays like

$$c(1 + \|\omega\|_2^2)^{-\tau} \leq \hat{\Phi}(\omega) \leq C(1 + \|\omega\|_2^2)^{-\tau} \quad \text{for all } \omega \in \mathbb{R}^d,$$

for some $C \geq c > 0$ and *smoothness order* $\tau > d/2$, which is an important parameter in convergence rate. This includes the Wendland compactly supported kernels [1] and the Sobolev kernel with smoothness order τ

$$\Phi_\tau(x, z) := \|x - z\|_{\ell^2(\mathbb{R}^d)}^{\tau - d/2} \mathcal{K}_{\tau - d/2}\big(\|x - z\|_{\ell^2(\mathbb{R}^d)}\big) \qquad \text{for } x, z \in \mathbb{R}^d, \tag{1}$$

where $\mathcal{K}$ Bessel functions of the second kind. Other commonly used kernels, such as, multiquadrics

$$\Phi(x, z) = \sqrt{\|x - z\|_{\ell^2(\mathbb{R}^d)}^2 + 1} \qquad \text{for } x, z \in \mathbb{R}^d,$$

and Gaussian

$$\Phi(x, z) = \exp\big(-\|x - z\|_{\ell^2(\mathbb{R}^d)}^2\big) \qquad \text{for } x, z \in \mathbb{R}^d,$$

remain useful in practice, but were not covered by the convergence theories below.

In Section 2, we will describe the well-known Kansa method [2] in order to introduce our notations to readers. In Sections 3 and 4, we will talk about two Kansa-type methods that can solve time-independent partial differential equations on surfaces. The last topic in Section 5 is to extend the projection method in Section 4 to solve time-dependent PDEs.

WIT Transactions on Engineering Sciences, Vol 134, © 2022 WIT Press
www.witpress.com, ISSN 1743-3533 (on-line)
doi:10.2495/BE450091

2 KANSA METHOD: A KERNEL BASED COLLOCATION METHOD

Let Ω be some nice (Ω is Lipschitz continuous and satisfies an interior cone condition.) *bulk* domain with a piecewise smooth boundary $\partial\Omega$. We consider a second-order elliptic equation

$$\begin{cases} \mathcal{L}u = f & \text{in } \Omega, \\ u = g & \text{on } \partial\Omega, \end{cases} \tag{2}$$

where $\mathcal{L}$ is a strongly elliptic operator with coefficients belonging to $W^{\tau}_{\infty}(\Omega)$, i.e., PDE coefficient functions in

$$\begin{aligned} \mathcal{L}u(x) \quad := \quad & \sum_{i,j=1}^{d} \frac{\partial}{\partial x^j}\left(a^{ij}(x)\frac{\partial}{\partial x^i}u(x)\right) + \sum_{j=1}^{d}\frac{\partial}{\partial x^j}\left(b^j(x)u(x)\right) \\ & + \sum_{i=1}^{d} c^i(x)\frac{\partial}{\partial x^i}u(x) + d(x)u(x), \end{aligned} \tag{3}$$

must have τ-bounded derivatives to go along with kernels with smoothness order τ and yield high order of convergence.

Let $Z = \{z_1, \ldots, z_{n_Z}\} \subset \overline{\Omega}$ be a set of n_Z trial centers (a.k.a., RBF centers). We can compute the *fill distance* of Z by

$$h_Z := \sup_{\zeta\in\Omega} \min_{z\in Z} \|z - \zeta\|_{\ell_2(\mathbb{R}^d)}, \tag{4}$$

and separation distance of Z by

$$q_Z := \frac{1}{2} \inf_{z_i \neq z_j \in Z} \text{dist}(z_i, z_j). \tag{5}$$

For any convergent method, we want the error to go to zero as $h_Z \to 0$. For numerical stability, we want to keep q_Z away from zero. One can use the *mesh ratio* $\rho_Z = h_Z/q_Z \geq 1$ to measure how "uniform" a given set of points is. We assume that Z is *quasi-uniform*, that is, the sequence of mesh ratios is bounded by a constant as we refine Z with increasing n_Z. We look for numerical approximation in the form of

$$u(x) = \sum_{j=1}^{n_Z} \lambda_j \Phi(x,\, z_j) \qquad \text{for } x \in \mathbb{R}^d. \tag{6}$$

As long as $\tau \geq 2$, then we can apply the differential operator $\mathcal{L}$ analytically to the x-variable of $\Phi(x, z)$ to yield $\Phi_{\mathcal{L}}(x, z)$. Now, let $X = \{x_1, \ldots, x_{n_X}\} \subset \Omega$ and $Y = \{y_1, \ldots, y_{n_Y}\} \subset \partial\Omega$ be sets of n_X and n_Y quasi-uniform collocation points in the interior and on the boundary that are dense enough with respect to Z with $n_X + n_Y > n_Z$. We are now ready to "collocate", that is, we put the ansatz (6) into (2) and then evaluate the resulting equations at all points in X and Y. The result is an $(n_X + n_Y) \times n_Z$ overdetermined system of equations:

$$\begin{bmatrix} \Phi_{\mathcal{L}}(x_1, z_1) & \cdots & \Phi_{\mathcal{L}}(x_1, z_{n_Z}) \\ \vdots & \ddots & \vdots \\ \Phi_{\mathcal{L}}(x_{n_X}, z_1) & \cdots & \Phi_{\mathcal{L}}(x_{n_X}, z_{n_Z}) \\ \hline \omega\,\Phi(y_1, z_1) & \cdots & \omega\,\Phi(y_1, z_{n_Z}) \\ \vdots & \ddots & \vdots \\ \omega\,\Phi(y_{n_Y}, z_1) & \cdots & \omega\,\Phi(y_{n_Y}, z_{n_Z}) \end{bmatrix} \begin{bmatrix} \lambda_1 \\ \vdots \\ \lambda_{n_Z} \end{bmatrix} = \begin{bmatrix} f(x_1) \\ \vdots \\ f(x_{n_X}) \\ \hline \omega\, g(y_1) \\ \vdots \\ \omega\, g(y_{n_Y}) \end{bmatrix},$$

where $\Phi_{\mathcal{L}}(x_i, z_j) = \mathcal{L}\Phi(x, z_j)|_{x=x_i}$, for some constant weight $\omega = h_Y^{d-4} h_X^{-d}$. If we allow functions and kernels to take set of points as input, we can use a more compact notation

$$\begin{bmatrix} \cdot & \Phi_{\mathcal{L}}(X, Z) & \cdot \\ \omega & \bar{\Phi}(\bar{Y}, \bar{Z}) & \cdot \end{bmatrix} \lambda = \begin{bmatrix} \cdot & f(X) & \cdot \\ \omega & g(\bar{Y}) & \cdot \end{bmatrix}. \tag{7}$$

Let λ_{LS} be the least-squares solution to (7), and with (6), the numerical approximation u_{LS} to the solution $u^* \in H^\tau(\Omega)$ of the PDE (2). Then, by [3, Thm. 2.6] (with $\theta = 2$, $\nu = 2$, $d \leq 3$), we know the following estimate holds up to $\mathbb{R}^3$

$$\|u_{LS} - u^*\|_{H^2(\Omega)} \leq C h_Z^{\tau-2} \|u^*\|_{H^\tau(\Omega)}. \tag{8}$$

if we use kernels with smoothness $\tau > 3 + d/2$.

3 EMBEDDED KANSA METHOD FOR SURFACE PDES

We move from bulk domain Ω to some smooth ($\mathcal{S}$ is a connected and complete Riemannian manifold of $\mathbb{R}^d$ such that it is of class $\mathcal{C}^{\tau+3/2}$ and satisfies the assumptions on bounded geometry and boundary regularity.) and closed surface $\mathcal{S}$, say, a sphere or an ellipsoid in $\mathbb{R}^3$. We consider general second order strongly elliptic partial differential equations

$$\mathcal{L}_{\mathcal{S}} u := (-a\Delta_{\mathcal{S}} + b \cdot \nabla_{\mathcal{S}} + c)u = f \quad \text{on } \mathcal{S} \subset \mathbb{R}^d, \tag{9}$$

where the surface differential operator $\mathcal{L}_{\mathcal{S}}$ has $W_\infty^{\tau-5/2}(\mathcal{S})$-bounded coefficients, i.e., $(\tau - 5/2)$-bounded derivatives as in the previous section. To define the surface Laplacian $\Delta_{\mathcal{S}}$, a.k.a. Laplace–Beltrami operator, we need the normal vector $n = n(p)$ at all $p \in \mathcal{S}$. For the unit sphere, for example, $n = [x, y, z]^T$. Then, the surface gradient $\nabla_{\mathcal{S}}$ and the surface Laplacian $\Delta_{\mathcal{S}}$ can be defined as

$$\nabla_{\mathcal{S}} := (I - nn^T)\nabla \quad \text{and} \quad \Delta_{\mathcal{S}} := \nabla_{\mathcal{S}} \cdot \nabla_{\mathcal{S}}, \tag{10}$$

using the standard Euclidean gradient ∇ and Laplacian Δ operators for $\mathbb{R}^d$. We want to avoid dealing with (10) by embedding the surface PDE (9) into a bulk domain. Consider a similar-looking PDE

$$\mathcal{L}w := (-a_{\text{cp}}\Delta + b_{\text{cp}} \cdot \nabla + c_{\text{cp}})w = f_{\text{cp}} \quad \text{in } \Omega_\delta \subset \mathbb{R}^d, \tag{11}$$

in some narrow-band (bulk) domain by

$$\Omega_\delta \quad = \quad \{x \in \mathbb{R}^d : \|x - \xi\|_{\ell_2(\mathbb{R}^d)} < \delta \text{ for some } \xi \in \mathcal{S}\}, \tag{12}$$

with coefficient $a_{\text{cp}} = a \circ \text{cp}$ where $\text{cp}(x) = \arg\inf_{\xi \in \mathcal{S}} \|\xi - x\|_{\ell^2(\mathbb{R}^d)}$ is the closest-point mapping [4]. For the unit sphere $\mathcal{S}$, we have $\text{cp}([3, 0, 0]^T) = [1, 0, 0]^T$, which is the point on $\mathcal{S}$ closest to the input. Also, $\text{cp}([0, 0, 0]^T)$ is undefined, meaning that we must take $\delta < 1$ in (12). For more complicated surfaces, the cp search can be done numerically. The other coefficient functions are defined by the same way.

The fact, without providing details, is that if w satisfies (11) and has a *constant-along-normal (CAN) property*, i.e., $w(p) = w(p \pm \epsilon n(p))$ for all $p \in \mathcal{S}$ and $\epsilon \leq \delta$, then restricting w on $\mathcal{S}$ solves the surface PDE (9), i.e., $u = w_{|\mathcal{S}}$.

Note that (9) is well-posed, but (11) is not, due to the missing boundary conditions. The discussion above is valid because we assume w is CAN, which can be made into *embedding*

conditions to make (11) well-posed. There are two options:

$$\begin{array}{ll} \text{(EC-I)} & \partial_n u := n^T \nabla u = 0 = \partial_n^{(2)} u := n^T J(\nabla u) n \quad \text{for all } p \in \mathcal{S}, \\ \text{(EC-II)} & u(p) = u(\mathrm{cp}(p)) \qquad\qquad\qquad\qquad\quad \text{for all } p \in \partial\Omega. \end{array} \tag{13}$$

If the bandwidth δ in (12) is small enough, (EC-II) is a good finite difference approximation to (EC-I). The embedded PDE (11) in Ω_δ with either one of the embedding conditions in (13) is now well-posed and can be solved by the least-squares Kansa method in Section 2. Since the problem domain is now Ω_δ, we chose quasi-uniform sets of RBF centers $Z \subset \Omega_\delta$ but sufficiently dense collocation points $X \subset \mathcal{S}$ with $h_X \leq \delta$. Orthogonal gradient method [5] is a popular way to generate X, in which data points are aligned along the normal of $\mathcal{S}$ that can speed up the implementation of EC-II.

The corresponding matrix systems for EC-I and EC-II are

$$\begin{bmatrix} \Phi_{\mathcal{L}}(X,Z) \\ \Phi_{\partial_n}(X,Z) \\ \Phi_{\partial_n^{(2)}}(X,Z) \end{bmatrix} \lambda = \begin{bmatrix} f(X) \\ \mathbf{0}(X) \\ \mathbf{0}(X) \end{bmatrix}, \tag{14}$$

and

$$\begin{bmatrix} \Phi_{\mathcal{L}}(X,Z) \\ \Phi(Z,Z) - \Phi(\mathrm{cp}(Z),Z) \end{bmatrix} \lambda = \begin{bmatrix} f(X) \\ \mathbf{0}(Z) \end{bmatrix}, \tag{15}$$

of sizes $3n_X \times n_Z$ and $(n_X + n_Z) \times n_Z$, respectively, where $\mathbf{0}$ stands for the zero function. The convergent embedded Kansa method indeed requires *both* embedding conditions in (13) in theory. The matrix system is in the form of (14) with EC-I appended with the second row of (15) for EC-II.

Here, we present a simplified version of convergence result, which is more stable numerically. Let λ_{LS} be the least-squares solution to the EC-I solution of (14), and with (6), the numerical approximation u_{LS} to the solution $u_{\mathcal{S}}^* \in H^{\tau-1/2}(\mathcal{S})$ of the surface PDE (9). Then, by [6, Thm. 4.1] (with $m = \tau - 1/2$, $k = 2$, $\delta = h_X$, $\epsilon \nearrow \infty$), the following estimate holds

$$\|u_{LS} - u_{\mathcal{S}}^*\|_{H^2(\mathcal{S})} \leq C\left(h_Z^{\tau-5/2-d/2} + h_X^{1/2} h_Z^{\tau-2-d/2}\right) \|u_{\mathcal{S}}^*\|_{H^{\tau-1/2}(\mathcal{S})}, \tag{16}$$

provided the smoothness order of kernel is $(\tau - 1/2) > d/2 + 7/2$. All the 0.5-order appeared in this paragraph are due to the trace theorem when our analysis goes between $\mathcal{S}$ and Ω_δ. We remark that it is common to observe higher than predicted in (16) rate of convergence numerically, since $\mathcal{S}$ used in numerical experiments are usually a lot nicer than the theoretical assumptions.

4 PROJECTION KANSA METHOD FOR SURFACE PDES

Let us consider the same surface PDE (9). In contrast to the embedded Kansa method, we want to work directly on the surface PDE. Thus, we also want on-surface RBF centers $Z \subset \mathcal{S}$ in this section. As usual, sets of collocation points $X \subset \mathcal{S}$ have to be sufficiently dense with respect to Z. With the numerical expansion in the form of (6), collocating the single governing equation in (9) yields an $n_X \times n_Z$ overdetermined simplest-ever matrix system

$$\begin{bmatrix} \Phi_{\mathcal{L}_{\mathcal{S}}}(X,Z) \end{bmatrix} \lambda = \begin{bmatrix} f(X) \end{bmatrix}. \tag{17}$$

Let λ_{LS} be the least-squares solution to (17), and with (6), the numerical approximation u_{LS} to the solution $u_{\mathcal{S}}^* \in H^{\tau-1/2}(\mathcal{S})$ of the surface PDE (9). Then, by [7, Thm. 1.1] (with

$m = \tau - 1/2$, $k = 2$), we have a much tidier error estimate

$$\|u_{LS} - u^*\|_{H^2(\mathcal{S})} \leq C h_Z^{\tau-2-d/2} \|u^*\|_{H^{\tau-1/2}(\mathcal{S})} \tag{18}$$

given $\tau - 1/2 - 1/2 \geq \lceil 5/2 + d/2 \rceil$. The price for all these simplicities is the trouble in evaluating the function $\Phi_{\mathcal{L}_\mathcal{S}}(\cdot, z)$.

When we have some parametric information about $\mathcal{S}$, it is possible to compute $\Phi_{\mathcal{L}_\mathcal{S}}$ analytically. Take the unit sphere as an example again. The projection matrix function $\mathcal{P}$ is given by

$$\begin{aligned} \mathcal{P}(p) &= \big[\mathcal{P}_1, \mathcal{P}_2, \mathcal{P}_3\big](p) \quad := \quad \big[I - nn^T\big](p) \\ &= \begin{bmatrix} -x^2+1 & -xy & -xz \\ -xy & -y^2+1 & -yz \\ -xz & -yz & -z^2+1 \end{bmatrix} \qquad \text{for } p = (x, y, z) \in \mathcal{S}. \end{aligned}$$

Then, we can use the definitions in (10) to compute surface gradient and surface Laplacian of any smooth function. Note that the latter involves differentiating normal vectors. Carrying out all calculation symbolically yields, for example,

$$\begin{aligned} \mathcal{L}_\mathcal{S} &= \Delta_\mathcal{S} - \mathbf{1} \cdot \nabla_\mathcal{S} \\ &= \Big((x-1)^2 + x(y+z) - 2\Big)\frac{\partial}{\partial x} + \Big((y-1)^2 + y(x+z) - 2\Big)\frac{\partial}{\partial y} \\ &\quad + \Big((z-1)^2 + z(x+y) - 2\Big)\frac{\partial}{\partial z} + \Big(-x^2+1\Big)\frac{\partial^2}{\partial x^2} + \Big(-y^2+1\Big)\frac{\partial^2}{\partial y^2} \\ &\quad + \Big(-z^2+1\Big)\frac{\partial^2}{\partial z^2} - 2xy\frac{\partial^2}{\partial x \partial y} - 2xz\frac{\partial^2}{\partial x \partial z} - 2yz\frac{\partial^2}{\partial y \partial z}, \end{aligned}$$

that can be used to compute $\Phi_{\mathcal{L}_\mathcal{S}}$ for the sake of collocation. Due to the large amount of exact analytic information in this method, this analytic-projection Kansa method is orders of magnitude more accurate than the embedded Kansa method in Section 3.

When we know $\mathcal{S}$ implicitly by some oriented point cloud Z with normal vectors $n(Z)$, we can employ a pseudospectral approach [8] to approximate the gradient of some function u based on its (known or unknown) function values at Z. Using the nodal values $u(Z)$, we can define the interpolant of u in the trial space $\mathcal{U}_Z := \text{Span}\{\Phi(\cdot, z_i) \big|\ z_i \in Z\}$ as

$$I_Z u(\cdot) = [\Phi(\cdot, Z)][\Phi(Z, Z)]^{-1} u(Z) \qquad \text{on } \mathcal{S}. \tag{19}$$

The surface gradient of u can then be approximated by

$$\begin{aligned} \nabla_\mathcal{S} u &\approx \nabla_\mathcal{S}(I_Z u) \\ &= \begin{bmatrix} \mathcal{P}_1^T \nabla \\ \vdots \\ \mathcal{P}_d^T \nabla \end{bmatrix} (I_Z u) = \begin{bmatrix} (\mathcal{P}_1^T \nabla)\Phi(\cdot, Z)[\Phi(Z, Z)]^{-1} \\ \vdots \\ (\mathcal{P}_d^T \nabla)\Phi(\cdot, Z)[\Phi(Z, Z)]^{-1} \end{bmatrix} u(Z) =: \begin{bmatrix} G_1(\cdot, Z) \\ \vdots \\ G_d(\cdot, Z) \end{bmatrix} u(Z), \end{aligned}$$

where $G_k(\cdot, Z) : \mathcal{S} \to \mathbb{R}^{1 \times n_Z}$ is a row-vector function. To avoid any confusion in notations, the operator $(\mathcal{P}_1^T \nabla) = [-x^2+1, -xy, -xz] \cdot [\partial_x, \partial_y, \partial_z]$ on the unit sphere and

$$(\mathcal{P}_1^T \nabla)\Phi(\cdot, Z) = \Big[(\mathcal{P}_1^T \nabla)\Phi(\cdot, z_1), \ldots, (\mathcal{P}_1^T \nabla)\Phi(\cdot, z_{n_Z})\Big],$$

is a row-vector function of length n_Z.

To avoid differentiating normal vectors, we can repeatedly apply the same pseudospectral idea to each component of $\nabla_{\mathcal{S}} u$ in order to approximate the surface Laplacian as

$$\Delta_{\mathcal{S}} u \approx \nabla_{\mathcal{S}} \cdot \vec{I}_Z\big(\nabla_{\mathcal{S}}(I_Z u)\big) = \sum_{k=1}^{d} G_k(\cdot, Z) G_k(Z, Z) u(Z) \qquad \text{on } \mathcal{S}.$$

The equality above is not that trivial and we refer readers to the original article for details. In terms of numerical accuracy, this pseudospectral-projection Kansa method is the second runner up among the three. Readers are referred to the numerical examples in Chen and Ling [7].

5 KANSA METHOD OF LINES FOR SURFACE DIFFUSION

Consider surface diffusion problem

$$\frac{\partial}{\partial t} u(x,t) + \Delta_{\mathcal{S}} u(x,t) = f(x,t) \quad \text{for } (x,t) \in \mathcal{S} \times [0,T] \tag{20}$$

$$u(x,0) = g(x) \qquad \text{for } x \in \mathcal{S}. \tag{21}$$

One can discretize in time first by some finite difference scheme to yield a sequence of surface elliptic PDEs, that can be solved by methods in Sections 3 and 4 or other localized meshless finite difference methods [9], [10].

In this section, we focus on the method of lines (MoL), in which we discretize in space first to (hopefully) yield ordinary differential equation (ODE) systems. Let us follow the standard steps in Kansa methods using on-surface RBF centers $Z \subset \mathcal{S}$ and collocation points $X \subset \mathcal{S}$. Putting the numerical expansion (6) into the governing eqn (20) and collocating at X yields

$$\Phi(X,Z)\, \frac{\partial}{\partial t} \lambda(t) + (\Delta_{\mathcal{S}} \Phi)(X,Z)\, \lambda(t) = f(X,t) \qquad \text{for } t \in [0,T]. \tag{22}$$

As long as $n_X > n_Z$, this is a differential algebraic equation (DAE) but not ODE. In Chen et al. [11], we show that the fully-discretized continuous-least-squares DAE solution can be approximated up to arbitrarily high order by the ODE solution

$$\dot{\lambda}(t) = \underbrace{-\Phi(X,Z)^{\dagger} (\Delta_{\mathcal{S}} \Phi)(X,Z)}_{\text{ODE matrix}}\, \lambda(t) + \Phi(X,Z)^{\dagger} f(X,t) \qquad \text{for } t \in [0,T], \tag{23}$$

where $\dagger$ denotes the pseduoinverse operator. Although (23) looks like the normal equation of (22), we emphasise that this intuition is not what's going on in the theoretical analysis. We can use (21) to obtain an initial condition $\lambda(0)$, say by interpolation or by a regularized least-squares approximation in Chen et al. [11, Sect. 3.4]. Let $\lambda_{LS}(t)$ be the solution to (23) subject to some $\mathcal{O}(h_Z^{\tau-2})$-convergent initial condition $\lambda_{LS}(0)$, then, by [11, Thm. 3.6 and Cor. 4.2] (with $m = \tau - 1/2$, $d_{\mathcal{S}} = d - 1$), the following estimate holds

$$\begin{aligned} \mathcal{E}(u_{LS} - u^*) \quad \leq \quad & C\Big(h_Z^{2\tau-4-d} \big(\|\dot{u}^*\|^2_{H^{\tau-5/2}(\mathcal{S})} + \|u^*\|^2_{H^{\tau-1/2}(\mathcal{S})} \big) \\ & + \big(h_Z^{2\tau-3} + h_X^{-2} h_Z^{2\tau-d} + h_X^{2\tau-3} \big) \|u^*(\cdot,0)\|^2_{H^{\tau-1/2}(\mathcal{S})} \Big) \end{aligned} \tag{24}$$

with error functional

$$\mathcal{E}(u) := \operatorname*{ess\,sup}_{0\le t\le T} \|u\|^2_{H^1(\mathcal{S})} + \|u\|^2_{L^2(0,T;H^1(\mathcal{S}))} + \|\dot{u}\|^2_{L^2(0,T;H^0(\mathcal{S}))}, \tag{25}$$

if the smoothness order of kernel is $\tau \ge \lfloor 5/2 + d/2 \rfloor$. This estimate also applies if $\Delta_{\mathcal{S}}$ is replaced by a more general second-order uniformly elliptic operator in divergence form

$$\mathcal{L}_{\mathcal{S}} u(y,t) := -\nabla_{\mathcal{S}} \cdot \big(A(y,t)\nabla_{\mathcal{S}} u(y,t)\big) \quad \text{for } (y,t) \in \mathcal{S} \times [0,T],$$

with some diffusion tensor A satisfying [11, Asm. 1].

Example: Consider a pure surface diffusion problem on a torus with zero initial condition $g = 0$ and a localized source function f, which is at the lower-left part of the surface as shown in Fig. 1. The ODE (23) with zero initial condition $\lambda(0) = \mathbf{0}(Z)$ can be solved by any black-box solver; in this demo, we use ODE45 in MATLAB to call a Runge–Kutta method for an adaptive integration.

Before we start solving ODEs, we need to ensure that the eigenvalues of the ODE matrix

$$-\Phi(X,Z)^{\dagger}(\Delta_{\mathcal{S}}\Phi)(X,Z)$$

in (23) are stable, i.e., no (large) real positive parts. We generate five sets of quasi-uniform data points with size 361, 784, 1156, 2916, and 5476. These sets were used as both RBF centers and collocation points. ODE matrices were generated using the Sobolev kernel in (1) with smoothness order $\tau - 1/2 = 6$ and 7.

Table 1 lists the maximum eigenvalues of these ODE matrix. We can clearly see the entries (in red) that ODE matrices with $X = Z$ can results in unstable eigenvalues. The need of oversampling, a.k.a., over-testing, with $n_X > n_Z$ is more evidential in this parabolic case than in elliptic. All cases with oversampling have maximum eigenvalues in ODE matrix very closed to zero (Spurious phenomenon due to the ill-conditioning problem of $\Phi(X,Z)$, i.e., factitious zero eigenvalues, were not considered.), some of them are positive that appears to be a random phenomenon due to rounding error. For very long time integration, users may consider applying some regularization.

Table 1: Maximum of eigenvalues of the ODE matrix associated with kernel with smoothness order $\tau = 6.5$ and $\tau = 7.5$. Cases with unstable eigenvalues are colored red for easy inspection.

		$n_X = 784$	1156	2916	5476
$\tau = 6.5$	$n_Z = 361$	1.00e-7	1.90e-7	2.91e-7	−1.79e-6
	784	4.87e-7	**−4.67e-6**	−1.27e-6	−1.59e-6
	1156		1.65e+4	1.80e-6	1.63e-6
$\tau = 7.5$	$n_Z = 361$	1.56e-4	9.27e-5	6.75e-5	5.32e-5
	784	5.05e+3	2.57e-4	2.79e-5	3.93e-5
	1156		8.28e+4	3.62e-5	5.74e-5

We pick the case $\tau = 6.5$, $n_Z = 784$ and $n_X = 1156$ to complete the solution process up to time $t = 10$. Two snapshots of the numerical solution are shown in Fig. 1. We report that all the other cases with stable eigenvalues generate simulations that are indistinguishable to the eyes.

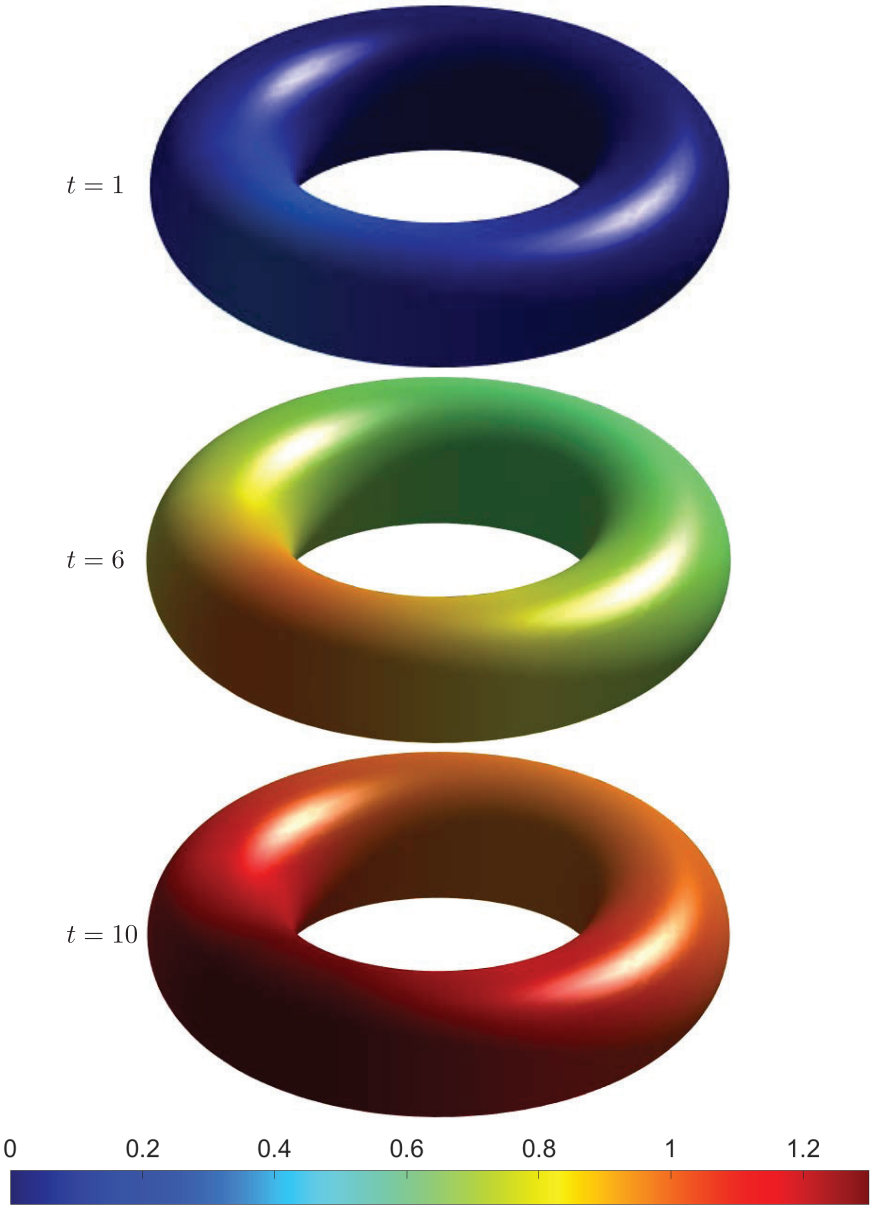

Figure 1: With $n_Z = 784$ and $n_X = 1156$, snapshots profiles, which use the same colormap for easy comparison, of the RBF ($\tau = 6.5$) MoL solutions to an isotropic diffusion reaction equation at various times.

6 CONCLUSION

Meshfree methods of any kind are good alternatives for solving PDEs on surfaces, on which data points are intrinsically scattered. It is well-known that the error of Kansa method concentrates near the boundary when we solve PDEs in bulk domain. Because there is no boundary in closed surfaces, all Kansa methods we reviewed in this paper shows faster than theoretical rate of convergence in practice. Although our presentation only covers linear PDEs, more interesting numerical examples (i.e., Turing pattern formations, spiral wave equation, Allen-Cahn, etc.) can be found in the references.

ACKNOWLEDGEMENTS

This work was supported by the Hong Kong Research Grant Council GRF Grants and the National Science Funds of China (Grant No. 12001261).

REFERENCES

[1] Wendland, H., Error estimates for interpolation by compactly supported radial basis functions of minimal degree. *Journal of Approximation Theory*, **93**(2), pp. 258–272, 1998.

[2] Kansa, E.J., Multiquadrics—A scattered data approximation scheme with applications to computational fluid-dynamics. I. Surface approximations and partial derivative estimates. *Computers & Mathematics with Applications*, **19**(8–9), pp. 127–145, 1990.

[3] Cheung, K.C., Ling, L. & Schaback, R., $\mathcal{H}^2$–convergence of least-squares kernel collocation methods. *SIAM Journal on Numerical Analysis*, **56**(1), pp. 614–633, 2018.

[4] Ruuth, S.J. & Merriman, B., A simple embedding method for solving partial differential equations on surfaces. *Journal of Computational Physics*, **227**(3), pp. 1943–1961, 2008.

[5] Piret, C., The orthogonal gradients method: A radial basis functions method for solving partial differential equations on arbitrary surfaces. *Journal of Computational Physics*, **231**(14), pp. 4662–4675, 2012.

[6] Cheung, K.C. & Ling, L., A kernel-based embedding method and convergence analysis for surfaces PDEs. *SIAM Journal on Scientific Computing*, **40**(1), pp. A266–A287, 2018.

[7] Chen, M. & Ling, L., Extrinsic meshless collocation methods for PDEs on manifolds. *SIAM Journal on Numerical Analysis*, **58**(2), pp. 988–1007, 2020.

[8] Fuselier, E.J. & Wright, G.B., A high-order kernel method for diffusion and reaction-diffusion equations on surfaces. *Journal of Scientific Computing*, **56**, pp. 535–565, 2013.

[9] Petras, A., Ling, L., Piret, C. & Ruuth, S., A least-squares implicit RBF-FD closest point method and applications to PDEs on moving surfaces. *Journal of Computational Physics*, **381**, pp. 146–161, 2019.

[10] Petras, A., Ling, L. & Ruuth, S., An RBF-FD closest point method for solving PDEs on surfaces. *Journal of Computational Physics*, **370**, pp. 43–57, 2018.

[11] Chen, M., Cheung, K.C. & Ling, L., A kernel-based least-squares collocation method for surface diffusion. arXiv: 2109.03409 [math.NA], 2021.